

**The *Caudal* ParaHox gene is required for hindgut development in the  
mollusc *Tritia* (a.k.a. *Ilyanassa*)**

Adam B. Johnson and J. David Lambert

Department of Biology, University of Rochester  
Rochester, NY USA 14627

Author for correspondence:  
J. David Lambert, [dlamber2@ur.rochester.edu](mailto:dlamber2@ur.rochester.edu)

## Abstract

Caudal homeobox genes are found across animals, typically linked to two other homeobox genes in what has been called the ParaHox cluster. These genes have been proposed to pattern the anterior-posterior axis of the endoderm ancestrally, but the expression of Caudal in extant groups is varied and often occurs in other germ layers. Here we examine the role of *Caudal* in the embryo of the mollusc *Tritia (Ilyanassa) obsoleta*. *ToCaudal* expression is initially broad, then becomes progressively restricted and is finally only in the developing hindgut (a.k.a. intestine). Knockdown of *ToCaudal* using morpholino oligonucleotides specifically blocks hindgut development, indicating that despite its initially broad expression, the functional role of *ToCaudal* is in hindgut patterning. This is the first functional characterization of *Caudal* in an animal with spiralian development, which is an ancient mode of embryogenesis that arose early in bilaterian animal evolution. These results are consistent with the hypothesis that the ancestral role of the ParaHox genes was anterior-posterior patterning of the endoderm.

## Introduction

The anterior-posterior (A-P) axis is the oldest animal axis and is recognizable in most animal groups. Bilaterian A-P axes are patterned by a genetically linked cluster of transcription factors called Hox genes (reviewed in McGinnis and Krumlauf, 1992). Famously, the gene expression of Hox genes exhibits spatial collinearity, in which the order of genes within the Hox cluster corresponds with

the anterior-posterior position of gene expression along the body axis (Lewis, 1978).

A smaller cluster of Hox-like genes, the ParaHox cluster, is present in metazoans but is less understood. Three linked genes comprise the ParaHox cluster—*Gsx*, *Xlox*, and *Cdx* (for *Caudal homeobox*). ParaHox gene expression from the leech, fly, frog, lancelet and mouse led to the hypothesis that, similar to the Hox cluster, ParaHox genes conferred A-P information to endoderm, with *Gsx* patterning the foregut, *Xlox* the midgut, and *Cdx* the hindgut (Brooke et al., 1998; Calleja et al., 1996; Duprey et al., 1988; Holland et al., 1997; Jonsson et al., 1994; Offield et al., 1996; Wysocka-Diller et al., 1995). This implied that the complex was active in endoderm of the bilaterian common ancestor (Holland, 2001). However, further work has shown that ParaHox gene expression domains do not fit this hypothesis in a simple way. For example, *Gsx* is not expressed in some animal foreguts but is expressed in anterior nervous system tissues (Garstang et al., 2016; Wollesen et al., 2015) and *Xlox* expression is also present in the nervous system of some deuterostomes (Levine and Schechter, 1993; Perillo et al., 2018). The posterior ParaHox gene *Caudal* seems to be most variable in its expression, and frequently appears in other germ layers across the Metazoa (Fig. 1). These varied expression patterns have complicated understanding of the ancestral function of *Caudal*, and the ancestral role of the ParaHox cluster in general.

Broadly speaking, there are five areas of *Caudal* expression in animals: endodermal hindgut, ectodermal hindgut, neural, posterior mesoderm, and

general posterior expression in multiple germ layers. Caudal's ancestral role is likely a subset of these. Caudal expression in these domains is patchy across bilaterian groups, indicating a complicated evolutionary history of co-options and/or losses (summarized in Fig. 1). Overall, the endodermal hindgut, and general posterior expression domains appear more frequently in the phylogeny, while neuroectoderm, ectodermal hindgut, and mesoderm are less frequent. Overall, the distribution of various expression domains across the phylogeny does not support any simple conclusion about the ancestral expression or role of Caudal (see references in Fig. 1 legend). Nevertheless, the data suggest two alternative hypotheses. First, Caudal may have been an ancestral hindgut gene, as suggested in (Holland, 2001), and underwent frequent co-option into other domains. Or, Caudal may have been broadly expressed in the posterior of the common ancestor, perhaps to confer posterior identity across germ layers. To resolve these questions will require functional studies with dense sampling from phylogenetically diverse organisms.

Thus far, Caudal functional studies are still rare, and typically confined to model organisms. In vertebrates Caudal paralogs are key regulators of posterior Hox genes, as Caudal mutations eliminate posterior axial growth (Chawengsaksophak et al., 2004; Neijs et al., 2017; Shimizu et al., 2005; Young et al., 2009). Suppressing *Caudal* function in an ascidian prevents larval tail extension (Katsuyama et al., 1999). In *D. melanogaster*, *Caudal* first specifies posterior identity and is later necessary for germband extension and hindgut formation (Macdonald and Struhl, 1986; Wu and Lengyel, 1998). In *C. elegans*, *Caudal* mutants show rectum and posterior muscle defects (Edgar et al., 2001).

Functional studies of Caudal (or other ParaHox genes) are entirely missing from one animal superphylum, the Spiralia.

The protostome clade Spiralia contains more than one-third of all extant bilaterian phyla but has received significantly less attention from developmental biologists, compared to the deuterostomes (e.g. vertebrates, ascidians and urchins) or ecdysozoans (e.g. arthropods and nematodes). Assessing gene function in the Spiralia is required for a reliable inference of Caudal's ancestral function and evolution. The expression of Caudal and other ParaHox genes have been examined in other spiralian, and a summary of expression domains for Caudal is shown in Fig. 1. In general, Caudal is frequently expressed in ectoderm and endoderm, and is observed in mesoderm in about half of the taxa examined. Functional tests have not been reported for any ParaHox gene in the Spiralia.

Here we investigate the expression pattern and functional role of *Caudal* in the development of the gastropod *Tritia* (formerly *Ilyanassa*), a useful model for studies of spiralian development, where no ParaHox genes have yet been characterized. The early development of *Tritia* and a simplified fate map is shown in Fig. 1B-I. Like many other spiralian, *Tritia*'s hindgut is generated from a blast cell lineage called the mesentoblast, which functions as a posterior growth zone by generating bilaterally paired bands of endodermal and mesodermal progenitor cells (See Fig. 2; Rabinowitz et al, 2008; Chan and Lambert, 2014). *Tritia obsoleta Caudal (ToCaudal)* is transiently expressed in the mesentoblast, as well as the putative hindgut precursors. It is also expressed in some ectodermal cells

in the developing foot. Zygotic knockdown of *ToCaudal* with a translation blocking morpholino oligo results in hindgut-less embryos. These results indicate that *ToCaudal* plays a specific role in posterior endoderm derived from a teloblastic growth zone in a gastropod.

## **Materials and Methods**

### *Snail husbandry and embryo collection*

Adult snails were collected from locations near Woods Hole, MA and Portland, ME, USA during late fall, winter and spring. Animal care and embryo collection have been described previously (Gharbiah et al. 2008). Egg capsules are laid on aquarium walls and harvested by scraping the glass with razor blades. Capsules are opened with iridectomy scissors and the embryos are gently removed by water expelled from a pulled glass pipette.

### *Tritia embryo fixation, counterstaining and visualization*

Hatching larvae were grown until they have depleted their maternally provided yolk deposits (about 10 days after egg laying). Larvae were then relaxed in TCB (Trichlorobutanol, Sigma)-saturated dH<sub>2</sub>O, 1:2 with 0.2 µm filtered artificial sea water (FASW) then fixed in PEM (100 mM PIPES [pH 6.9], 10 mM EGTA, 1 mM MgSO<sub>4</sub>, and 0.1% Triton-X 100, paraformaldehyde (Polysciences) and 75 mM sucrose overnight at 4°C, followed by three washes in PBTw (1x PBS; 0.1% Tween). Embryos and pre-hatching larvae (ranging from zygote to around 5 days old) do not require relaxation and were fixed as above. DNA was stained with DAPI (1 µg/mL in 80% glycerol; 1x PBS; Molecular Probes). Embryos and

larvae were imaged with a Zeiss Axioplan 2 for brightfield and fluorescent imaging.

#### ToCaudal cloning and *in situ* hybridization

A fragment of *ToCaudal* was originally identified in an EST screen, and extended using 5' RACE-PCR. The *in situ* probe preparation was performed as in Kingsley et al. 2007. The *ToCaudal* probe is 378bp long and amplified from cDNA with forward (5'-TAATACGACTCACTATAGGGAGAAACCCATCTCCATGCTG-3') and reverse (5'-AATTAACCCTCACTAAAGGGAGCCGCTACTCCTCCTCTTC-3') primers which include T7 or T3 sequences, respectively, for sense or antisense probe transcription. *In situ* hybridization was performed as in Kingsley et al. 2007. Briefly, embryos were fixed with PEM (0.1M Pipes, 2mM EGTA, 1 mM MgSO<sub>4</sub>, 4% paraformaldehyde) for at least two hours. Embryos were pretreated for 10 min in 2% acetic anhydride in TEA (triethanolamine) and prehybridized for 3 h at 68°C in Hyb solution (5x SSC, 1x Denharts, 50% formamide, 1% Tween20, 100µg ml<sup>-1</sup> heparin and 100 µg ml<sup>-1</sup> yeast rRNA plus tRNA), hybridized with digoxigenin-labelled probe for 72 h, washed four times over 2 h with Hyb solution at 68°C. Chromogenic *in situ*s were detected by nitro blue tetrazolium/5-bromo-4-chloro-3-indoyl phosphate chemistry. For all patterns reported, at least 15 embryos from at least 3 sets of synchronously cleaving embryos (i.e. egg capsules) were examined, and the pattern was consistent between them. The cell assignments were made from stacks of optical sections and while looking at the embryos at 400X, and the images we present are projections using Helicon Focus software (Helicon Soft Ltd., Ukraine).

### *Knockdowns, rescue, and overexpression*

*ToCaudal*MO (5'- GAGAAGAAACCCATCTCCATGCTGG-3'), was designed for translational blocking by Gene Tools (Philomath Oregon). The control morpholino (5'- TCCATGTCAGTGTCCAAGCC-3') was designed for a previous project; the Standard Control morpholino also gives no phenotype in this embryo (Rabinowitz and Lambert, 2010). Morpholinos were diluted with dH<sub>2</sub>O and Sulforhodamine 101 dye (Molecular Probes (250 ng/μl) and filtered by Costar filters (Corning). Injections were performed as in Gharbiah et al. 2008 by zygotic injection using Femtotip needles (Eppendorf). For mRNA production, the *ToCaudal* ORF was cloned into pCS2P+ using BamHI and PstI sites. RNA was synthesized with an Sp6-Scribe Standard RNA IVT kit and capped and tailed with the mScript Standard mRNA Production kit (both Cellscript). The resulting mRNA lacks *ToCaudal*MO's 5' UTR binding site. Rescue and overexpression solution was prepared as above; *ToCaudal* mRNA (250 ng/μl) was injected with 0.66mM *ToCaudal*MO for rescue and *ToCaudal* mRNA at 250 ng/μl for overexpression. After injection embryos were transferred into FASW in 35mm Corning Falcon tissue media dishes. Dishes were placed into empty pipette tip boxes with moistened paper towels to maintain humidity. Unless otherwise noted, all experiments were performed with at least 15 embryos from at least three capsules, which contain a synchronously cleaving clutch of embryos.

## **Results**

### *ToCaudal expression*

*ToCaudal* mRNA is initially broadly expressed during early cleavage, in both the 2<sup>nd</sup> and 3<sup>rd</sup> quartets at the 28-cell stage (Fig. 2A-D). It is also present in the mesentoblast cell 4d, which generates a posterior teloblast lineage that undergoes stereotyped cell divisions to generate mesoderm and some endoderm. Previous 4d lineage tracing has shown that this lineage gives rise to the hindgut (a.k.a. intestine; Chan and Lambert, 2014; Render, 1997). 4d divides to give rise to the bilaterally paired mesentoblast mother cells ML and MR. After these cells divide once, *ToCaudal* is weakly expressed in the first mesentoblast daughters 1mL and 1mR (Fig. 2E-H). *ToCaudal* is also expressed in seven cells from the lineage of the 2d micromere that overlie the 4d lineage. From this point, the mesentoblast continues dividing to produce bilaterally symmetrical daughter cells. The four most vegetal pairs of daughters (1mL and 1mR; 2mL and 2mR; 3mL and 3mR; 4mL and 4mR; 5mL and 5mR) express *Caudal* immediately after their births. These are the hindgut precursors, based on lineage tracing from a related gastropod (Conklin, 1897; Lyons et al., 2012); consistent with that, in this system they appear to maintain expression through organogenesis as they develop into the hindgut. There are five *ToCaudal*-expressing ectodermal cells above the 4d lineage; three 2d cells flanked by 2a<sup>211</sup> and 2c<sup>121</sup> (Fig. 2I-L); collectively, these second quartet cells will generate various ectodermal structures like shell, proximal foot, and stomodeum, as well as some ganglia. Three of these cells divide once more around the 5ML and R stage, then lose expression sometime during gastrulation. After gastrulation at three days old, *ToCaudal* is found in 12-15 sub-ectodermal cells at the ventral posterior and in two ectodermal regions, each comprised of two cells, in the lateral sides of the

developing foot (white arrowheads; Fig. 2Q). The ectodermal domains disappear before the 4 day old stage (Fig. 2R), and the posterior group of cells moves to the dorsal right side of the embryo during the process of torsion, and forms the hindgut (Fig. 2S; Chan and Lambert, 2014; Tomlinson, 1987). In the veliger larva the hindgut connects the style sac to the anus and retains *ToCaudal* expression (Fig. 2T).

#### *ToCaudal* knockdown

To test the role of *ToCaudal* in development we obtained a translation-blocking morpholino oligonucleotide (MO) targeting *ToCaudal* (*ToCaudal*MO) (Fig. 3C-D). We injected *ToCaudal*MO into zygotes at concentrations from 0.33mM to 1.33mM and found that the only consistent defect was an absence of all or part of the hindgut; this effect was dose dependent, with the presence of wildtype hindgut ranging from 100% at 0.33mM to 0% at 1.33mM (Table 1). At 1.33 mM, all structures were at least mildly impacted, even those, like the eyes and head, whose progenitor cells (1abcd) do not express *ToCaudal*. This indicates that there were some non-specific effects of the morpholino at this concentration. We therefore focused on animals injected with 0.66 mM, where less than 18% of animals had normal hindguts, and other structures we scored were essentially wildtype. The hindgut is always strongly pigmented, and its nuclei are arranged in a distinctive tube shape. We know of no other marker genes that are specific to the hindgut—other than the *ToCaudal* mRNA itself in later stages. However, the distinctive morphology and pigmentation of this organ make it very straightforward to score its presence or absence conclusively. The other

structures of the gut, including the stomach, style sac and esophagus, were not affected.

We observed no phenotypes that could be associated with the paired ectodermal clusters on the embryo's ventral side. These clusters appear to lie in the 3c and 3d clones (Chan and Lambert, 2014), which give rise to the left and right halves of the foot. We do not see any defects in the ectoderm, pedal gland or muscle system of the foot. The paired pedal ganglia also arise from this general region (Dickinson and Croll, 2003); we could see apparently normal numbers and arrangement of nuclei in the developing ganglia, based on DAPI staining in whole mounts. Finally, we note that despite *ToCaudal*'s expression in the posterior cells of the mesentoblast lineage we observe no phenotypes in other 4d derivatives that we scored, *viz.* the heart and larval retractor muscle. The kidney also derives from 4d (see confocal stacks in Chan and Lambert, 2014). We do not normally score this organ because it can collapse in fixation leading to false negatives. However, *ToCaudal* knockdown animals seemed to generally have kidneys (e.g. Fig. 3D). This further supports the idea that *ToCaudal* function in the 4d lineage is specific to the hindgut.

Embryos injected with a control morpholino were wildtype, indicating that the phenotypes we observe are not due to injection or morpholino toxicity. To further demonstrate the specificity of the MO phenotype, we injected *ToCaudal*/MO with a *Tritia Caudal* mRNA lacking the morpholino target sequence (Fig 3. E-F). Co-injection of 0.66mM *ToCaudal*/MO and 125 ng/μl *ToCaudal* mRNA resulted in most animals having partial (3/22) or full hindguts (15/22),

indicating partial rescue of the phenotype (Table 1). Injection of 125 ng/μl *ToCaudal* mRNA alone had no effect on hindgut size or location and we observed no ectopic hindgut cells, suggesting that *ToCaudal* mRNA alone is not sufficient to redirect other cells to hindgut fates (Table 1).

We wondered if the absence of hindgut after *ToCaudal*/MO knockdown was due to abnormal 4d teloblast divisions, as is the case with *Nanos* knockdown (see Fig. 2 left column and Rabinowitz et al., 2008). We injected 0.66mM *ToCaudal*/MO into zygotes and fixed at the 4MLR (~84 cell) stage and the 5MLR (~97cell) stage. As expected, in 4MLR control embryos, each 4d teloblast had produced four daughters (Fig. 4A). *ToCaudal*/MO-injected embryos had correctly positioned 1, 3, and 4mLR cells, as well as wildtype 2<sup>nd</sup> quartet cell positions (Fig. 4B). In 5MLR control embryos, each mesentoblast had produced five daughters (Fig. 4C). *ToCaudal*/MO-injected embryos had correctly positioned 1, 3, 4, and 5mL and R cells and wildtype 2<sup>nd</sup> quartet cell positions (Fig. 4D). These experiments show that hindgut loss in *ToCaudal*/MO animals is not associated with an irregular 4d teloblast cleavage pattern.

In a further attempt to understand the cause of the hindgut defect, we then compared *ToCaudal* knockdown and control embryos later, after gastrulation. There are many subectodermal cells in the region of the hindgut precursors (as in Fig. 2R), and we were unable to conclusively determine if there was a difference in this population after knockdown by looking at the DAPI stained embryos. The only marker we have for these cells is *ToCaudal* mRNA itself; the morpholino is predicted to block translation, but we reasoned that if *ToCaudal* protein were required for subsequent *ToCaudal* transcription, or if *ToCaudal*-

expressing cells were absent, there might be fewer *ToCaudal* mRNA-positive cells after knockdown. We injected 0.66 mM *ToCaudal*MO and fixed embryos after three days (a similar stage to Fig. 2R), then performed *ToCaudal* *in situ* hybridization. We DAPI stained these animals and examined embryos at high power to tally the number of *ToCaudal* positive cells. After *ToCaudal*MO injection we observed a significant decrease in the number of *ToCaudal* positive hindgut precursor cells compared to uninjected control embryos ( $p < 5e-22$ ; *t*-test; Fig. 5) as well as loss of the paired ectodermal foot domains. Since there are fewer *ToCaudal* positive cells in knockdown embryos at this stage (0-4 cells) than there are putative hindgut precursors in 5MLR-stage (8 cells), this suggests that, after translational knockdown, *ToCaudal* expression is being lost, and/or cell death is occurring.

Together with the results in Figure 4, this indicates that the putative hindgut precursor cells are born normally, but without *ToCaudal* activity they die or lose *ToCaudal* mRNA expression. This occurs during the interval between these stages, when the population of caudal positive cells in the hindgut primordium normally goes from 8 to 16. This is in contrast to an alternative scenario where knockdown was preventing proliferation after the 5MLR stage.

We note that, while the loss of *ToCaudal* mRNA expression is not necessarily predicted after knockdown, it is unlikely to be observed due to an off-target effect and thus further supports the specificity of the phenotype.

## **Discussion:**

The most posterior ParaHox gene, Caudal, has long been considered to have a conserved role in the development of the posterior of animal body plans.

However, its diverse expression patterns across the Metazoa have complicated our understanding of exactly where and how Caudal functioned in the bilaterian ancestor, and the role of the ParaHox genes in general. In the present study we have performed the first *Caudal* knockdown in the Spiralia and found that it is required for development of the hindgut in a mollusc. This apparently simple phenotype contrasts with the complex patterns of expression across animals (See Figure 1 and references therein), and in this embryo itself, where *Caudal* is expressed in a variety of lineages in ectoderm and endoderm, at least early in development.

### *Caudal in spiralian endoderm and mesentoblast lineages*

*ToCaudal* is required for posterior endoderm development in *Tritia*'s mesentoblast lineage. The gene is expressed in the 1<sup>st</sup>, 3<sup>rd</sup>, 4<sup>th</sup>, and 5<sup>th</sup> daughters of the mesentoblast, the precise set that generate hindgut in the related snail *Crepidula fornicata* (Lyons et al., 2012), and not in any other 4d daughters that we can detect. This, together with the specific effects of *ToCaudal* knockdown on the hindgut, indicates that *ToCaudal* functions specifically in the posterior, endoderm-generating cells of the 4d lineage in this embryo. Caudal is expressed in 4d-derived hindgut in other molluscs like *Antalis*, *Acanthochitona*, *Gibbula*, and *Crepidula*, indicating that this role was ancestral for molluscs (Fritsch et al., 2016; Perry et al., 2015; Samadi and Steiner, 2010; Wollesen et al., 2018).

The 4d contribution to both mesoderm and endoderm is conserved in many spirilians, but the specific contribution to hindgut is less common. 4d does make mesoderm and endoderm in the nemertean *Cerebratulus lacteus*, but this contribution is not specific to the hindgut (Henry and Martindale, 1998; Boyer et al., 1996). Descriptive studies in multiple polychaetes have reported minor contributions of the 4d lineage to the posterior midgut (reviewed in Anderson, 1973). In the polychaete annelids *Capitella teleta* and *Platynereis dumerilii*, modern lineage-tracing methods have shown that the 4d lineage does not generate any endoderm, but it does make a set of primordial germ cells that might have been confused with endodermal cells in previous studies (Ackermann et al., 2005; Meyer and Seaver, 2010, Rebscher et al., 2012; see also Fischer and Arendt, 2013 and Özpolat et al., 2017, though these are cell lineage studies that do not follow lineages long enough to determine their tissue contribution).

In the leech *Helobdella* (sp.) the 4d lineage (called DM'') was found to produce some anterior endoderm, in addition to its well-known role producing segmental mesoderm (Gline et al., 2011). One interpretation of the absent or less pronounced role of the 4d lineage in making endoderm in annelids is that the lineage shifted to function more in the production of mesoderm concomitantly with the evolution of the elaborate segmented muscle system in polychaetes. Overall, the available evidence indicates that in the spiralian common ancestor, 4d made mesoderm and endoderm, but the latter contribution was not necessarily limited to hindgut, as in molluscs.

The role of Caudal in hindgut development is more conserved across spiralian than the contribution of 4d to the hindgut. In addition to the molluscs referenced above, both *Platynereis* and *Capitella* express Caudal in their hindguts, even though these tissues derive from ectoderm, not 4d. Consistent with this, ancestral genes identified as core endomesodermal genes pattern *Capitella* gut into regions regardless of which germ layer these cells arose from (Boyle et al., 2014), and a gradient of *Caudal* expression extends from the ectodermal hindgut into the endodermal midgut in *Nereis virens* (Kulakova et al., 2008). In two nemerteans, Caudal expression was found in the ectoderm and endodermal components of the developing hindgut (Hiebert and Maslakova, 2015; Martín-Durán et al., 2015). In the related phyla Brachiopoda and Phoronida, which are members of the group Lophophorata, the spiral cleavage program has been variously modified, so that the homology of the 4d cell has not been established (see Pennerstorfer and Scholtz, 2012). Nevertheless, Caudal is expressed in the developing hindgut endoderm and ectoderm in these taxa (Andrikou et al., 2019). The phyla Ectoprocta (or Bryozoa) is a third representative of the Lophophorata. Intriguingly, it has recently been reported that in the embryo of the ectoproct *Membranipora membranacea*, the spiral cleavage program has been modified, but it is possible to recognize cells that are homologous with a typical spiralian embryo, including 4d. In this embryo 4d does express *Caudal*, and while the fate of 4d could not be determined in this study, the developing hindgut does express *Caudal* at a later stage (Vellutini et al., 2017). These results indicate that Caudal is involved in hindgut development in this embryo, and suggest that there could be a direct contribution of 4d to hindgut

in this lophophorate. Together, these results show that Caudal expression in the developing hindgut is strongly conserved in the Spiralia, and is more tightly linked to hindgut identity than endodermal identity. As mentioned above, platyhelminth flatworms have a ‘blind gut’, comprised of foregut and midgut, but no hindgut. Surprisingly, this phylum seems to be the only bilaterian phylum that has lost *Caudal* from its genome (Martín-Durán and Romero, 2011). The fact that *Caudal* was lost, perhaps concomitantly with the loss of the hindgut in this lineage, hints that *Caudal* had no other essential functions in the ancestor-- indirect evidence that Caudal functioned specifically in hindgut in the spiralian ancestor.

#### *Caudal in the bilaterian ancestor*

If Caudal functioned specifically in the hindgut in the spiralian ancestor, then this increases the likelihood of that role in the urbilaterian. However, the alternative is still possible—an ancestral role as a broadly expressed posterior positional identity factor. The data from bilaterian outgroups cannot clearly discern between these two scenarios. ParaHox (and Hox) genes are absent from the genome of the ctenophore *Mnemiopsis leidyi* (Ryan et al., 2013), and there are no clear ParaHox genes in sponges (Finnerty et al., 2004; Fortunato et al., 2014; Pastrana et al., 2019; Ryan et al., 2010) , which may not even have germ layers as we typically understand them (Nakanishi et al., 2014). The placozoan *Trichoplax adherens* gene *Trox-2* seems to be an ortholog of the ParaHox gene Gsx and it is expressed broadly on the bottom epithelium, which is similar to endoderm or mouth (DuBuc et al., 2019). Cnidarians have clear ParaHox genes but it remains uncertain whether any have a bilaterian-like triple cluster. In the

anemone *Nematostella vectensis*, there are two linked genes, one that is orthologous with *Gsx* and one that is related to *Xlox* and/or *Cdx* (Chourrout et al., 2006; Ryan et al., 2007). The coral *Acropora digitifera* has only a *Gsx* gene (DuBuc et al., 2012). Surprisingly, in jellyfish there are three ParaHox genes in a cluster, including a clear *Gsx* ortholog and two other genes that are similar to *Xlox* and *Cdx* (Khalturin et al., 2019; Nong et al., 2020). The expression patterns of cnidarian *Cdx*-like ParaHox genes are also diverse. In *Nematostella*, the gene that is similar to *Cdx* and *Xlox* is expressed in cells that will become two mesenteries, which are flap-like partitions running along the primary axis of the gut. It is thus an endodermal expression pattern, but the two developing mesenteries where it is expressed are on one side of the secondary or directive axis (Ryan and Baxevanis, 2007). Thus, this gene does not have a clearly posterior expression pattern as in bilaterians. Recently, it was shown that some Hox genes in this animal function to subdivide the endoderm along the secondary axis (He et al., 2018), so the axial patterning role of those hox genes is parallel to that of the *Cdx*-like gene. In the jellyfish *Aurelia*, the gene that is most similar to *Cdx* is expressed in the gastrovascular system of the endoderm but was not reported to be restricted along either axis (Khalturin et al., 2019). More genomic, expression, and functional studies from additional diverse prebilaterian taxa will be necessary to infer when *Cdx* arose and what its ancestral function was.

The expression of *ToCaudal* is initially very broad and encompasses posterior ectoderm (2d lineage), and posterior endoderm and mesoderm (4d

lineage). During gastrulation, this broad domain resolves to a much more specific pattern in the hindgut precursors. In our knockdowns, we saw no effects on the development of ectodermal structures that derive from 2d, like the shell or the tip of the foot, or from mesodermal derivatives of 4d. We also found no defects in the foot, where small groups of ectodermal cells express *ToCaudal* during organogenesis. This suggests that the functional effects of *ToCaudal* are significantly narrower than its expression in this system. If the ancestral role of Caudal was specific to the hindgut, it could have evolved more broad functional roles in the posterior from a situation like we observe here, by the evolution of novel expression of Caudal in the posterior mesoderm and ectoderm. This would lead to Caudal functions similar to what are currently observed in insects and vertebrates.

### **Acknowledgments**

The authors thank Longjun Wu, Kim Thao Dao, and members of the Brisson lab for thoughtful discussions about this work. We are also grateful for the comments from two anonymous reviewers which greatly improved this manuscript. This work was supported by grants by the N.S.F. to J.D.L (IOS-1656558 and IOS-1146782).

## Tables and Figures:

Percentage of animals with wild-type development of the indicated larval organs

	from the 4d mesentoblast										n
	Ectoderm					Endoderm					
	Eyes	Velar lobes	Shell	Foot mass	Operculum	Style sac	Dig. gland	Stomach	Hindgut	Heart	Retractor muscle
.66mM Control MO	100	100	100	100	100	100	100	100	100	100	100
.33mM <i>ToCaudal</i> MO	100	100	100	100	100	100	100	100	100	100	100
.66mM <i>ToCaudal</i> MO	97	97	100	100	100	100	100	100	18*	100	100
1.33mM <i>ToCaudal</i> MO	90	90	90	90	90	90	90	90	0	90	90
.66mM <i>ToCaudal</i> MO + 125 ng/µL <i>ToCaudal</i> mRNA	100	100	100	100	100	95	95	90	68*	100	100
125 ng/µL <i>ToCaudal</i> mRNA	80	90	100	100	100	100	95	95	100	95	95

Table 1: Phenotype scoring of *ToCaudal* knockdown, rescue, and overexpression. All experiments used embryos from at least three capsules. Asterisks indicate partial hindguts: 2/33 0.66mM *ToCaudal* MO animals and 3/22 rescue animals had distal hindgut fragments, that were between 1/10-1/3th the length of the wildtype hindgut.

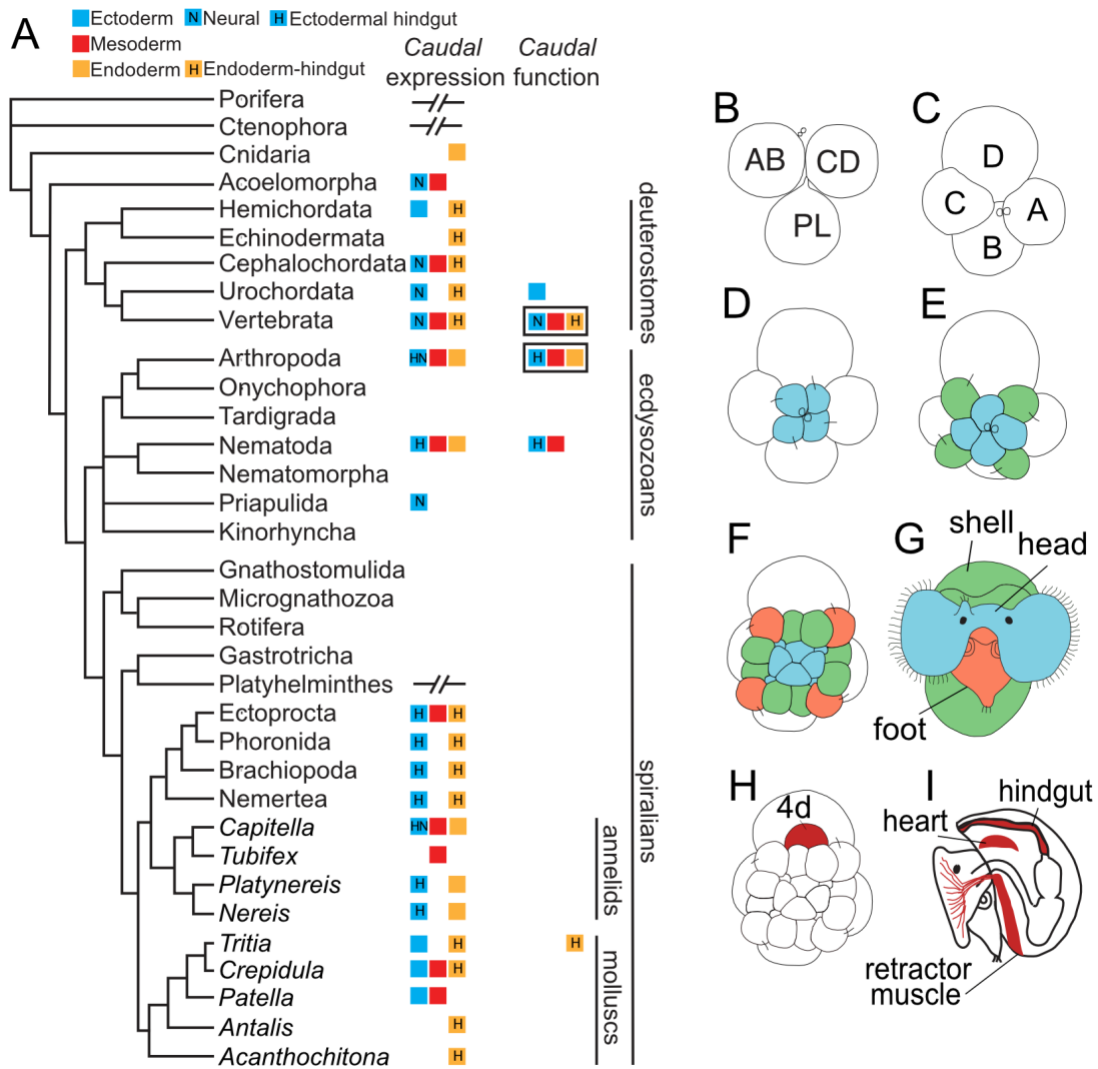


**Fig. 1: Phylogenetic distribution of Caudal studies.** A summary of Caudal gene expression and functional analyses in the Metazoa. Left, a consensus phylogeny of animals, compiled across multiple sources. Center column, *Caudal Expression*: Colored squares indicate the germ layers where Caudal expression has been reported; ectoderm is blue, mesoderm is red, and endoderm is orange. Phyla with no squares are missing data, taxa where Caudal has been sought but appears to absent based on genomic sequence data are indicated by double slashes (for Porifera and Ctenophora this is based on Ryan et al 2010; Pastrana et al, 2019; but see Fortunato et al, 2014). Hindgut is indicated with H, and neural structures with N. Right column, *Caudal function*: blue, red, and orange squares

represent reports of *Caudal* function in ectodermal, mesodermal, or endodermal structures, respectively. Boxes indicate phenotypes likely attributed to *Caudal*'s role as a posterior marker. (Altenburger et al., 2011; Annunziata and Arnone, 2014; Arnone et al., 2006; Beck et al., 1995; Brooke et al., 1998; Chawengsaksophak et al., 2004; Chesebro et al., 2012; Cole et al., 2009; Copf et al., 2004; Edgar et al., 2001; Fortunato et al., 2014; Fritsch et al., 2016; Fröbius and Seaver, 2006; Gao et al., 2009; Gonzalez et al., 2017; He et al., 2018; Hejnol and Martindale, 2008; Hiebert and Maslakova, 2015; Hinman et al., 2000; Hui et al., 2009; Ikuta et al., 2013; Katsuyama et al., 1999; Kulakova et al., 2008; Le Gouar et al., 2003; Leininger et al., 2014; Martín-Durán and Romero, 2011; Martín-Durán et al., 2012; Matsuo et al., 2005; McGregor et al., 2008; Nakao, 2010; Olesnický et al., 2006; Pastrana et al., 2019; Perry et al., 2015; Pillemer et al., 1998; Rabet et al., 2001; Rosa et al., 2005; Ryan et al., 2010; Shimizu et al., 2005; Shinmyo et al., 2005; Skromne et al., 2007; Smith et al., 2016; Wollesen Tim et al., 2018; Wu and Lengyel, 1998; Young et al., 2009). B-I) The early embryo of *Tritia (Ilyanassa) obsoleta*. B) The polar lobe is produced at the first cleavage (side view, animal pole up). C) The D macromere of the four-cell stage is specified by inheritance of the polar lobe (C-F and H are animal pole views with the dorsal side up). (D-F) Successive cleavage cycles produce the first quartet (D, blue), second quartet (E, green), and third quartet (F, light orange). G) Simplified fate map of the ectoderm in a veliger larva (anterior view with dorsal up). First quartet cells generate the head (blue); the second quartet generates the shell and posterior ectoderm (green); third quartet generates the foot and esophagus (orange). For more complete fate map information see Chan and Lambert 2014. H) The D macromere's fourth daughter is 4d, the mesentoblast (red), which is born before the other 4<sup>th</sup> quartet cells to make the 28 cell stage. I) The mesentoblast generates the hindgut, heart, larval retractor muscle and some cells in the head (left view, dorsal is up, anterior is facing left).

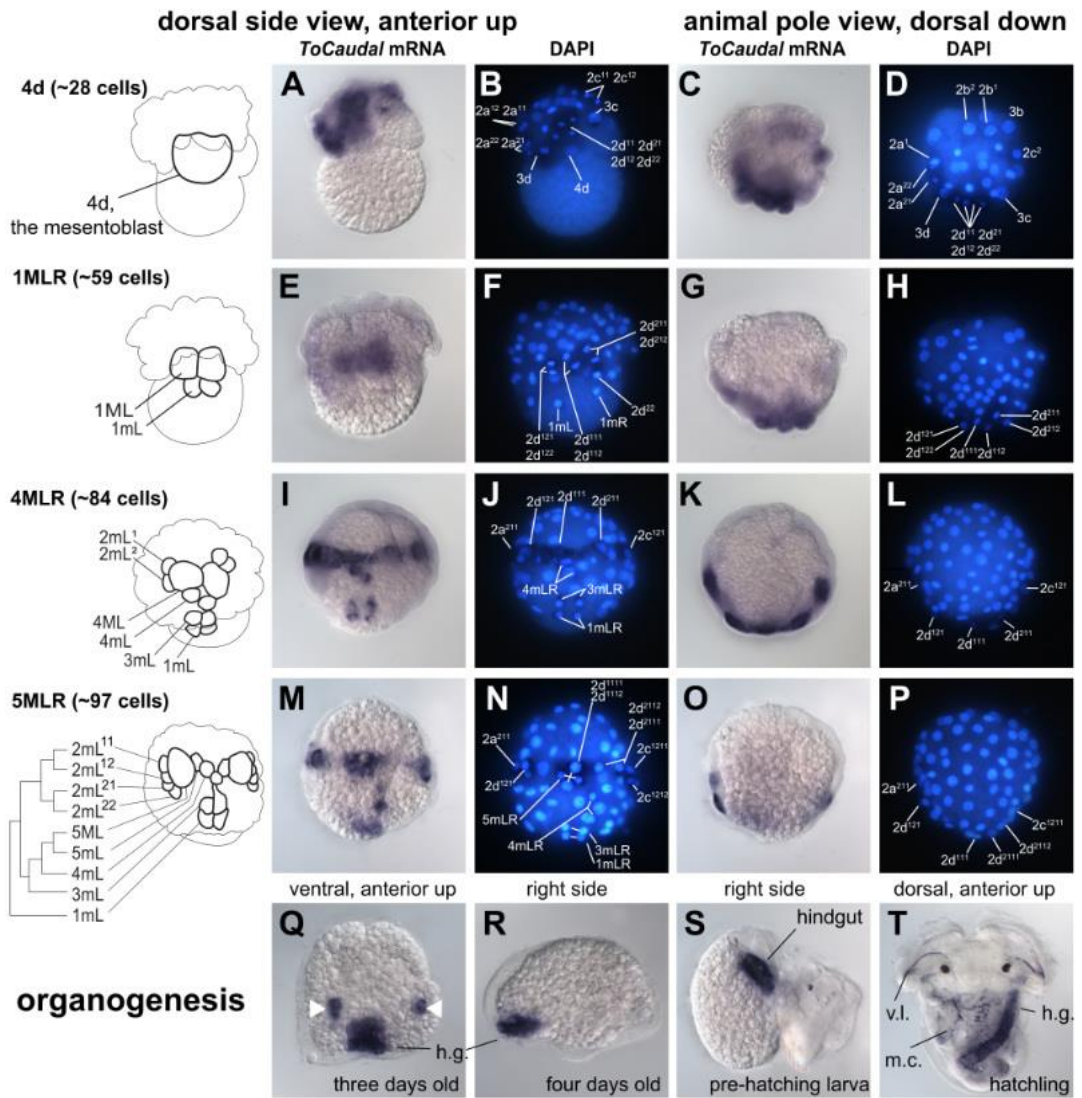


Fig. 2. *ToCaudal* expression during development. The first four rows correspond to the stages indicated, named for the mesentoblast cells at particular division cycles, and diagrams of the 4d lineage at those stages are on the left. (Note that, by convention, the 4d lineage is shown in dorsal view with animal pole up and, so the drawings and images in the first three columns are inverted relative to the early embryo diagrams in Figure 1.) (A-D) At the 28-cell stage, after the mesentoblast cell 4d is born, *ToCaudal* is expressed in the 2<sup>nd</sup> and 3<sup>rd</sup> quartets (i.e. 2abcd and 3abcd), as well as more weakly in 4d. (E-H) After the teloblasts (now called 1ML and 1MR) generate their first daughter cells, 1mL and R, *ToCaudal* message is weakly expressed in 1mL and R and in seven overlying 2d

cells ( $2d^{121}$ ,  $2d^{122}$ ,  $2d^{111}$ ,  $2d^{112}$ ,  $2d^{211}$ ,  $2d^{212}$ , and  $2d^{22}$ ). (I-L) After four divisions, the teloblasts are called 4ML and R, and *ToCaudal* is still expressed in  $2a^{211}$ ,  $2d^{121}$ ,  $2d^{111}$ ,  $2d^{211}$ , and  $2c^{121}$ , and in the six most vegetal 4d progeny (1,3,4 mL and R). (M-P) After one more teloblast division (5ML and R; ca. 90 cells) expression is still observed in  $2a^{211}$  and  $2d^{121}$ ; there are six other second quartet cells expressing *ToCaudal*, which are likely the daughters of  $2d^{111}$ ,  $2d^{211}$ , and  $2c^{121}$ :  $2d^{1111}$ ,  $2d^{1112}$ ,  $2d^{2111}$ ,  $2d^{2112}$ ,  $2d^{1211}$  and  $2c^{1212}$ . The eight vegetal teloblast progeny (1,3,4,5mL and R) continue to express *ToCaudal*. (Q) After gastrulation, in a three-day-old embryo, *ToCaudal* expression is found in bilaterally symmetrical pairs of ectodermal cells (white arrowheads) on the ventral surface and in a subectodermal cluster of cells at the posterior ventral portion of the embryo that will develop into the hindgut (h.g.). (R) In a four-day-old embryo, the subectodermal cluster has extended anteriorly, and will soon rotate to lie on the larva's dorsal right side, while the ectodermal staining has disappeared. (S) Pre-hatching veliger larvae, right side, anterior faces right. After torsion, the developing hindgut is on the dorsal right side of the developing mantle cavity (m.c.). (T) Hatchling veliger larvae, dorsal view, anterior is up. *ToCaudal* is specifically expressed in the hindgut (dorsal-right) indicating that the subectodermal cluster in Q, R, S are the hindgut primordium. m.c. marks the mantle cavity and v.l the velar lobes. Panels A-S are 260  $\mu$ m square, T is 290  $\mu$ m square.

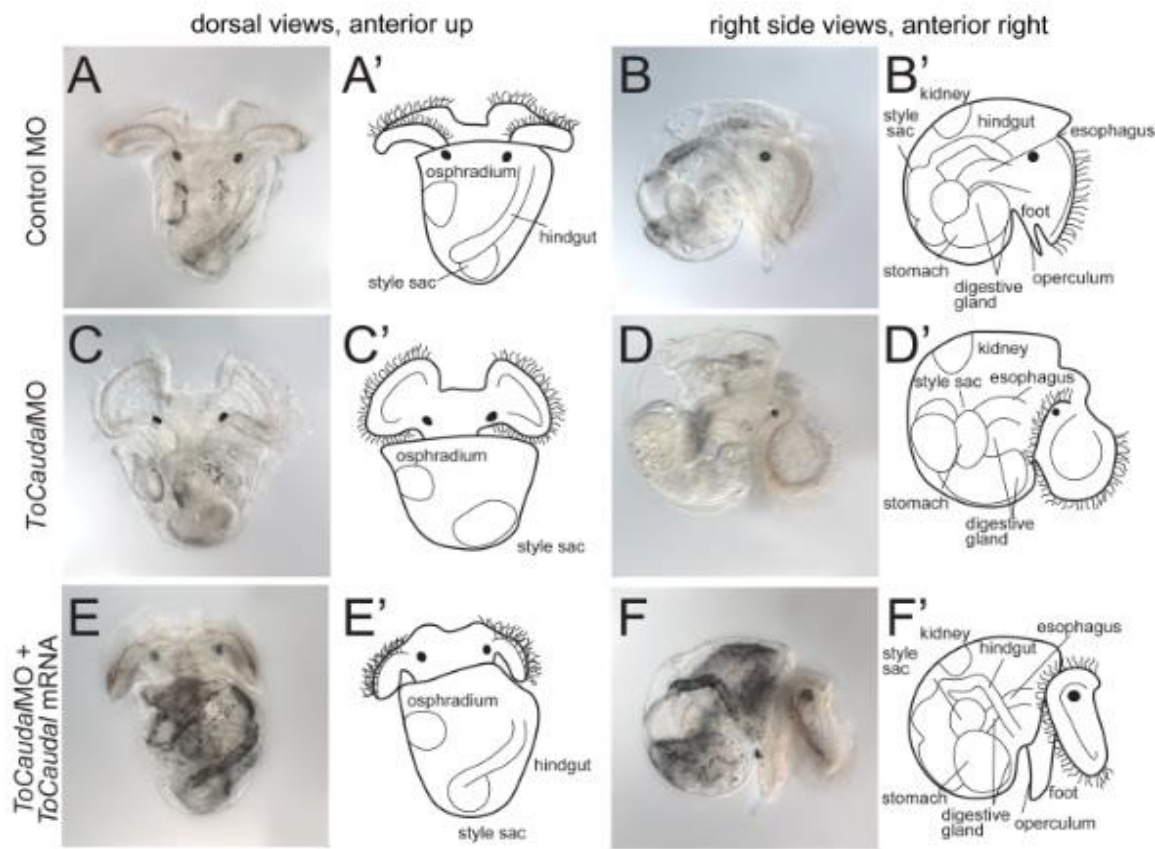


Fig. 3: *ToCauda*/MO phenotypes. (A, A') Veliger larva after injection of a control morpholino into zygotes; these animals are wildtype and have conspicuously pigmented hindguts running from the dorsal posterior to anterior right. (B, B') Right view of control larva; hindgut runs from style sac to anus on the right side, just behind the head. (C, C') Veliger larva, after injection of 0.66mM *ToCauda*/MO into the zygote; these animals lack hindgut but are otherwise wild type (see Table 1 for detailed scoring.) (D, D') Veliger from *ToCauda*/MO injection, right view (foot is out of plane but wildtype). (E, E') Veliger larva after coinjection of 0.66mM *ToCauda*/MO and 250 ng/ $\mu$ L *ToCaudal* mRNA has a wildtype hindgut. (F, F') As in E, E' but right view. Photo panels are 375  $\mu$ m square.

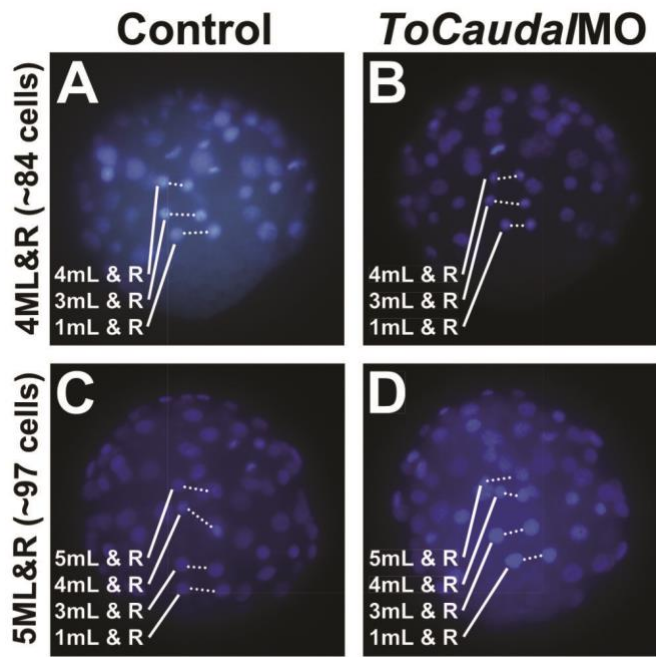


Fig. 4: Mesentoblast proliferation after *ToCauda* knockdown. After injecting *ToCauda*/MO and allowing development until 4MLR (similar to Fig. 2I-L) we stained with DAPI and assessed the number and position of *ToCauda* positive cells. (A) Control embryos have undergone four teloblast divisions; contralaterally paired progeny cells are connected with dotted lines. (B) *ToCauda*/MO injected embryos (0.66mM) were similarly staged (e.g. 2d<sup>112</sup> is in metaphase, above labeled cells in both) and produced 1, 3, and 4mLR similar to control embryos. (C) After one more teloblast division, around 4 hours later, control embryos have eight vegetal 4d daughters (1, 3, 4, and 5mLR). (D) *ToCauda*/MO injected animals have normally positioned 1, 3, 4, and 5mLR cells. All panels are 230  $\mu$ m square.

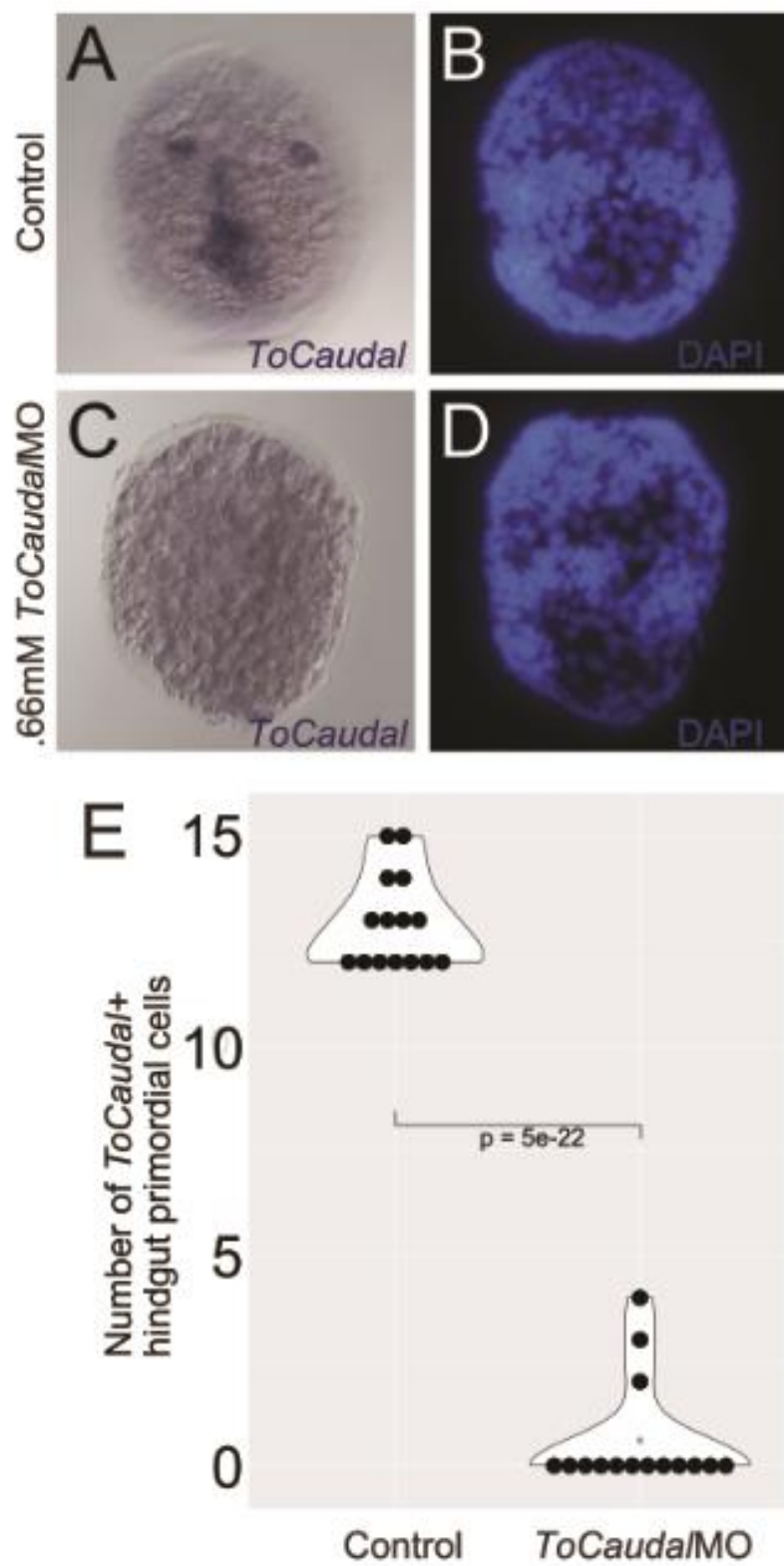


Fig. 5: *ToCaudal* organogenesis expression is lost after knockdown. After injecting *ToCaudal*MO into zygotes at 0.66mM we grew embryos to four-days-old and performed *in situ* hybridization for *ToCaudal*. (A) Uninjected control embryos expressed *ToCaudal* in a cluster of 12-15 subectodermal cells in the ventral posterior region (the hindgut primodium), and in paired two-cell ectodermal clusters in the foot. (B) Nuclear staining with DAPI of A. (C) After zygotic injection of 0.66 mM *ToCaudal*MO, embryos lacked *ToCaudal* expression. (D) Nuclear staining with DAPI of C. (E) Uninjected control embryos averaged 12.9 hindgut primordium cells with *ToCaudal* expression, while *ToCaudal*MO embryos averaged 0.6 *ToCaudal* expressing hindgut primordium cells. Each black dot represents a scored individual embryo. Counts of *ToCaudal* positive cells were compared by an unpaired *t*-test. Panels A-D are 260uM square.

## References cited

Ackermann, C., Dorresteijn, A., and Fischer, A. (2005). Clonal domains in postlarval *Platynereis dumerilii* (Annelida: Polychaeta). *J. Morphol.* **266**, 258–280.

Altenburger, A., Martinez, P., and Wanninger, A. (2011). Homeobox gene expression in Brachiopoda: the role of *Not* and *Cdx* in bodyplan patterning, neurogenesis, and germ layer specification. *Gene Expr. Patterns GEP* **11**, 427–436.

Anderson, D.T. (1973). CHAPTER 2 - POLYCHAETES. In *Embryology and Phylogeny in Annelids and Arthropods*, D.T. Anderson, ed. (Pergamon), pp. 7–50.

Andrikou, C., Passamaneck, Y.J., Lowe, C.J., Martindale, M.Q., and Hejnol, A. (2019). Molecular patterning during the development of *Phoronopsis harmeri* reveals similarities to rhynchonelliform brachiopods. *EvoDevo* **10**, 33.

Annunziata, R., and Arnone, M.I. (2014). A dynamic regulatory network explains ParaHox gene control of gut patterning in the sea urchin. *Development* **141**, 2462–2472.

Arnone, M.I., Rizzo, F., Annunziata, R., Cameron, R.A., Peterson, K.J., and Martínez, P. (2006). Genetic organization and embryonic expression of the ParaHox genes in the sea urchin *S. purpuratus*: Insights into the relationship between clustering and colinearity. *Dev. Biol.* **300**, 63–73.

Beck, F., Erler, T., Russell, A., and James, R. (1995). Expression of *Cdx-2* in the mouse embryo and placenta: possible role in patterning of the extra-embryonic membranes. *Dev. Dyn. Off. Publ. Am. Assoc. Anat.* **204**, 219–227.

Boyer, B.C., Henry, J.Q., and Martindale, M.Q. (1996). Dual origins of mesoderm in a basal spiralian: cell lineage analyses in the polyclad turbellarian *Hoploplana inquilina*. *Dev. Biol.* **179**, 329–338.

Boyle, M.J., Yamaguchi, E., and Seaver, E.C. (2014). Molecular conservation of metazoan gut formation: evidence from expression of endomesoderm genes in *Capitella teleta* (Annelida). *EvoDevo* **5**, 39.

Brooke, N.M., Garcia-Fernández, J., and Holland, P.W.H. (1998). The ParaHox gene cluster is an evolutionary sister of the Hox gene cluster. *Nature* **392**, 920–922.

Calleja, M., Moreno, E., Pelaz, S., and Morata, G. (1996). Visualization of gene expression in living adult *Drosophila*. *Science* **274**, 252–255.

Chan, X.Y., and Lambert, J.D. (2014). Development of blastomere clones in the *Ilyanassa* embryo: transformation of the spiralian blastula into the larval body plan. *Dev. Genes Evol.* **224**, 159–174.

Chawengsaksophak, K., Graaff, W. de, Rossant, J., Deschamps, J., and Beck, F. (2004). *Cdx2* is essential for axial elongation in mouse development. *Proc. Natl. Acad. Sci. U. S. A.* **101**, 7641–7645.

Chesbro, J.E., Pueyo, J.I., and Couso, J.P. (2012). Interplay between a Wnt-dependent organiser and the Notch segmentation clock regulates posterior development in *Periplaneta americana*. *Biol. Open* **BIO20123699**.

Chourrout, D., Delsuc, F., Chourrout, P., Edvardsen, R.B., Rentzsch, F., Renfer, E., Jensen, M.F., Zhu, B., de Jong, P., Steele, R.E., et al. (2006). Minimal ProtoHox cluster inferred from bilaterian and cnidarian Hox complements. *Nature* **442**, 684–687.

Cole, A.G., Rizzo, F., Martinez, P., Fernandez-Serra, M., and Arnone, M.I. (2009). Two ParaHox genes, *SpLox* and *SpCdx*, interact to partition the posterior endoderm in the formation of a functional gut. *Development* **136**, 541–549.

Conklin, E.G. (1897). The embryology of *crepidula*, A contribution to the cell lineage and early development of some marine gasteropods. *J. Morphol.* **13**, 1–226.

Copf, T., Schröder, R., and Averof, M. (2004). Ancestral role of caudal genes in axis elongation and segmentation. *Proc. Natl. Acad. Sci. U. S. A.* **101**, 17711–17715.

DuBuc, T.Q., Ryan, J.F., Shinzato, C., Satoh, N., and Martindale, M.Q. (2012). Coral comparative genomics reveal expanded Hox cluster in the cnidarian-bilaterian ancestor. *Integr. Comp. Biol.* **52**, 835–841.

DuBuc, T.Q., Ryan, J.F., and Martindale, M.Q. (2019). “Dorsal–Ventral” Genes Are Part of an Ancient Axial Patterning System: Evidence from *Trichoplax adhaerens* (Placozoa). *Mol. Biol. Evol.* **36**, 966–973.

Duprey, P., Chowdhury, K., Dressler, G.R., Balling, R., Simon, D., Guenet, J.L., and Gruss, P. (1988). A mouse gene homologous to the *Drosophila* gene *caudal* is expressed in epithelial cells from the embryonic intestine. *Genes Dev.* **2**, 1647–1654.

Edgar, L.G., Carr, S., Wang, H., and Wood, W.B. (2001). Zygotic Expression of the caudal Homolog *pal-1* Is Required for Posterior Patterning in *Caenorhabditis elegans* Embryogenesis. *Dev. Biol.* **229**, 71–88.

Finnerty, J.R., Pang, K., Burton, P., Paulson, D., and Martindale, M.Q. (2004). Origins of Bilateral Symmetry: *Hox* and *Dpp* Expression in a Sea Anemone. *Science* **304**, 1335–1337.

Fischer, A.H.L., and Arendt, D. (2013). Mesoteloblast-like mesodermal stem cells in the polychaete annelid *Platynereis dumerilii* (Nereididae). *J. Exp. Zool. B Mol. Dev. Evol.* **320**, 94–104.

Fortunato, S.A.V., Adamski, M., Ramos, O.M., Leininger, S., Liu, J., Ferrier, D.E.K., and Adamska, M. (2014). Calcisponges have a ParaHox gene and dynamic expression of dispersed NK homeobox genes. *Nature* *514*, 620–623.

Fritsch, M., Wollesen, T., and Wanninger, A. (2016). Hox and ParaHox gene expression in early body plan patterning of polyplacophoran mollusks. *J. Exp. Zoolog. B Mol. Dev. Evol.* *326*, 89–104.

Fröbius, A.C., and Seaver, E.C. (2006). ParaHox gene expression in the polychaete annelid *Capitella* sp. I. *Dev. Genes Evol.* *216*, 81–88.

Gao, N., White, P., and Kaestner, K.H. (2009). Establishment of Intestinal Identity and Epithelial-Mesenchymal Signaling by *Cdx2*. *Dev. Cell* *16*, 588–599.

Garstang, M.G., Osborne, P.W., and Ferrier, D.E.K. (2016). TCF/Lef regulates the *Gsx* ParaHox gene in central nervous system development in chordates. *BMC Evol. Biol.* *16*, 57.

Gline, S.E., Nakamoto, A., Cho, S.-J., Chi, C., and Weisblat, D.A. (2011). Lineage analysis of micromere 4d, a super-phylotypic cell for Lophotrochozoa, in the leech *Helobdella* and the sludge worm *Tubifex*. *Dev. Biol.* *353*, 120–133.

Gonzalez, P., Uhlinger, K.R., and Lowe, C.J. (2017). The Adult Body Plan of Indirect Developing Hemichordates Develops by Adding a Hox-Patterned Trunk to an Anterior Larval Territory. *Curr. Biol.* *27*, 87–95.

He, S., Viso, F. del, Chen, C.-Y., Ikmi, A., Kroesen, A.E., and Gibson, M.C. (2018). An axial Hox code controls tissue segmentation and body patterning in *Nematostella vectensis*. *Science* *361*, 1377–1380.

Hejnol, A., and Martindale, M.Q. (2008). Acoel development indicates the independent evolution of the bilaterian mouth and anus. *Nature* *456*, 382–386.

Henry, J.J., and Martindale, M.Q. (1998). Conservation of the spiralian developmental program: cell lineage of the nemertean, *Cerebratulus lacteus*. *Dev. Biol.* *201*, 253–269.

Hiebert, L.S., and Maslakova, S.A. (2015). Expression of Hox, *Cdx*, and *Six3/6* genes in the hoplonemertean *Pantinonemertes californiensis* offers insight into the evolution of maximally indirect development in the phylum Nemertea. *EvoDevo* *6*.

Hinman, V.F., Becker, E., and Degnan, B.M. (2000). Neuroectodermal and endodermal expression of the ascidian *Cdx* gene is separated by metamorphosis. *Dev. Genes Evol.* *210*, 212–216.

Holland, P.W. (2001). Beyond the Hox: how widespread is homeobox gene clustering? *J. Anat.* *199*, 13–23.

Holland, L.Z., Kene, M., Williams, N.A., and Holland, N.D. (1997). Sequence and embryonic expression of the amphioxus engrailed gene (*AmphiEn*): the metameric pattern of transcription resembles that of its segment-polarity homolog in *Drosophila*. *Development* 124, 1723–1732.

Hui, J.H., Raible, F., Korchagina, N., Dray, N., Samain, S., Magdelenat, G., Jubin, C., Segurens, B., Balavoine, G., Arendt, D., et al. (2009). Features of the ancestral bilaterian inferred from *Platynereis dumerilii* ParaHox genes. *BMC Biol.* 7, 43.

Ikuta, T., Chen, Y.-C., Annunziata, R., Ting, H.-C., Tung, C., Koyanagi, R., Tagawa, K., Humphreys, T., Fujiyama, A., Saiga, H., et al. (2013). Identification of an intact ParaHox cluster with temporal colinearity but altered spatial colinearity in the hemichordate *Ptychodera flava*. *BMC Evol. Biol.* 13, 129.

Jonsson, J., Carlsson, L., Edlund, T., and Edlund, H. (1994). Insulin-promoter-factor 1 is required for pancreas development in mice. *Nature* 371, 606.

Katsuyama, Y., Sato, Y., Wada, S., and Saiga, H. (1999). Ascidian Tail Formation Requires *caudal* Function. *Dev. Biol.* 213, 257–268.

Khalturin, K., Shinzato, C., Khalturina, M., Hamada, M., Fujie, M., Koyanagi, R., Kanda, M., Goto, H., Anton-Erxleben, F., Toyokawa, M., et al. (2019). Medusozoan genomes inform the evolution of the jellyfish body plan. *Nat. Ecol. Evol.* 3, 811–822.

Kulakova, M.A., Cook, C.E., and Andreeva, T.F. (2008). ParaHox gene expression in larval and postlarval development of the polychaete *Nereis virens* (Annelida, Lophotrochozoa). *BMC Dev. Biol.* 8, 61.

Le Gouar, M., Lartillot, N., Adoutte, A., and Vervoort, M. (2003). The expression of a *caudal* homologue in a mollusc, *Patella vulgata*. *Gene Expr. Patterns* 3, 35–37.

Leininger, S., Adamski, M., Bergum, B., Guder, C., Liu, J., Laplante, M., Bråte, J., Hoffmann, F., Fortunato, S., Jordal, S., et al. (2014). Developmental gene expression provides clues to relationships between sponge and eumetazoan body plans. *Nat. Commun.* 5, 3905.

Levine, E.M., and Schechter, N. (1993). Homeobox genes are expressed in the retina and brain of adult goldfish. *Proc. Natl. Acad. Sci.* 90, 2729–2733.

Lewis, E.B. (1978). A gene complex controlling segmentation in *Drosophila*. *Nature* 276, 565–570.

Lyons, D.C., Perry, K.J., Lesoway, M.P., and Henry, J.Q. (2012). Cleavage pattern and fate map of the mesentoblast, 4d, in the gastropod *Crepidula*: a hallmark of spiralian development. *EvoDevo* 3, 21.

Macdonald, P.M., and Struhl, G. (1986). A molecular gradient in early *Drosophila* embryos and its role in specifying the body pattern. *Nature* 324, 537–545.

Martín-Durán, J.M., and Romero, R. (2011). Evolutionary implications of morphogenesis and molecular patterning of the blind gut in the planarian *Schmidtea polychroa*. *Dev. Biol.* **352**, 164–176.

Martín-Durán, J.M., Janssen, R., Wennberg, S., Budd, G.E., and Hejnol, A. (2012). Deuterostomic Development in the Protostome *Priapulus caudatus*. *Curr. Biol.* **22**, 2161–2166.

Martín-Durán, J.M., Vellutini, B.C., and Hejnol, A. (2015). Evolution and development of the adelphophagous, intracapsular Schmidt's larva of the nemertean *Lineus ruber*. *EvoDevo* **6**, 28.

Matsuo, K., Yoshida, H., and Shimizu, T. (2005). Differential expression of *caudal* and *dorsal* genes in the teloblast lineages of the oligochaete annelid *Tubifex tubifex*. *Dev. Genes Evol.* **215**, 238–247.

McGinnis, W., and Krumlauf, R. (1992). Homeobox genes and axial patterning. *Cell* **68**, 283–302.

McGregor, A.P., Pechmann, M., Schwager, E.E., Feitosa, N.M., Kruck, S., Aranda, M., and Damen, W.G.M. (2008). *Wnt8* Is Required for Growth-Zone Establishment and Development of Opisthosomal Segments in a Spider. *Curr. Biol.* **18**, 1619–1623.

Meyer, N.P., and Seaver, E.C. (2010). Cell Lineage and Fate Map of the Primary Somatoblast of the Polychaete Annelid *Capitella teleta*. *Integr. Comp. Biol.* **50**, 756–767.

Nakanishi, N., Sogabe, S., and Degnan, B.M. (2014). Evolutionary origin of gastrulation: insights from sponge development. *BMC Biol.* **12**, 26.

Nakao, H. (2010). Characterization of *Bombyx* embryo segmentation process: expression profiles of *engrailed*, *even-skipped*, *caudal*, and *wnt1/wingless* homologues. *J. Exp. Zool. B Mol. Dev. Evol.* **314B**, 224–231.

Neijts, R., Amin, S., van Rooijen, C., and Deschamps, J. (2017). *Cdx* is crucial for the timing mechanism driving colinear Hox activation and defines a trunk segment in the Hox cluster topology. *Dev. Biol.* **422**, 146–154.

Nong, W., Cao, J., Li, Y., Qu, Z., Sun, J., Swale, T., Yip, H.Y., Qian, P.Y., Qiu, J.-W., Kwan, H.S., et al. (2020). Jellyfish genomes reveal distinct homeobox gene clusters and conservation of small RNA processing. *Nat. Commun.* **11**, 3051.

Offield, M.F., Jetton, T.L., Labosky, P.A., Ray, M., Stein, R.W., Magnuson, M.A., Hogan, B.L., and Wright, C.V. (1996). *PDX-1* is required for pancreatic outgrowth and differentiation of the rostral duodenum. *Dev. Camb. Engl.* **122**, 983–995.

Olesnicky, E.C., Brent, A.E., Tonnes, L., Walker, M., Pultz, M.A., Leaf, D., and Desplan, C. (2006). A *caudal* mRNA gradient controls posterior development in the wasp *Nasonia*. *Development* **133**, 3973–3982.

Özpolat, B.D., Handberg-Thorsager, M., Vervoort, M., and Balavoine, G. (2017). Cell lineage and cell cycling analyses of the 4d micromere using live imaging in the marine annelid *Platynereis dumerilii*. *ELife* 6, e30463.

Pastrana, C.C., DeBiase, M.B., and Ryan, J.F. (2019). Sponges Lack ParaHox Genes. *Genome Biol. Evol.* 11, 1250–1257.

Pennerstorfer, M., and Scholtz, G. (2012). Early cleavage in *Phoronis muelleri* (Phoronida) displays spiral features. *Evol. Dev.* 14, 484–500.

Perillo, M., Paganos, P., Mattiello, T., Cocurullo, M., Oliveri, P., and Arnone, M.I. (2018). New Neuronal Subtypes With a “Pre-Pancreatic” Signature in the Sea Urchin *Stonylocentrotus purpuratus*. *Front. Endocrinol.* 9.

Perry, K.J., Lyons, D.C., Truchado-Garcia, M., Fischer, A.H.L., Helfrich, L.W., Johansson, K.B., Diamond, J.C., Grande, C., and Henry, J.Q. (2015). Deployment of regulatory genes during gastrulation and germ layer specification in a model spiralian mollusc *Crepidula*. *Dev. Dyn.* 244, 1215–1248.

Pillemer, G., Epstein, M., Blumberg, B., Yisraeli, J.K., De Robertis, E.M., Steinbeisser, H., and Fainsod, A. (1998). Nested expression and sequential downregulation of the *Xenopus caudal* genes along the anterior-posterior axis. *Mech. Dev.* 71, 193–196.

Rabet, N., Gibert, J.-M., QuÉinnec, É., Deutsch, J.S., and Mouchel-Vielh, E. (2001). The *caudal* gene of the barnacle *Sacculina carcinis* is not expressed in its vestigial abdomen. *Dev. Genes Evol.* 211, 172–178.

Rabinowitz, J.S., and Lambert, J.D. (2010). Spiralian quartet developmental potential is regulated by specific localization elements that mediate asymmetric RNA segregation. *Development* 137, 4039–4049.

Rabinowitz, J.S., Chan, X.Y., Kingsley, E.P., Duan, Y., and Lambert, J.D. (2008). *Nanos* Is Required in Somatic Blast Cell Lineages in the Posterior of a Mollusk Embryo. *Curr. Biol.* 18, 331–336.

Rebscher, N., Lidke, A.K., and Ackermann, C.F. (2012). Hidden in the crowd: primordial germ cells and somatic stem cells in the mesodermal posterior growth zone of the polychaete *Platynereis dumerillii* are two distinct cell populations. *EvoDevo* 3, 9.

Render, J. (1997). Cell Fate Maps in the *Ilyanassa obsoleta* Embryo beyond the Third Division. *Dev. Biol.* 189, 301–310.

Rosa, R., Prud'homme, B., and Balavoine, G. (2005). *Caudal* and *even-skipped* in the annelid *Platynereis dumerilii* and the ancestry of posterior growth. *Evol. Dev.* 7, 574–587.

Ryan, J.F., and Baxevanis, A.D. (2007). Hox, Wnt, and the evolution of the primary body axis: insights from the early-divergent phyla. *Biol. Direct* 2, 37.

Ryan, J.F., Mazza, M.E., Pang, K., Matus, D.Q., Baxevanis, A.D., Martindale, M.Q., and Finnerty, J.R. (2007). Pre-Bilaterian Origins of the Hox Cluster and the Hox Code: Evidence from the Sea Anemone, *Nematostella vectensis*. PLOS ONE 2, e153.

Ryan, J.F., Pang, K., Mullikin, J.C., Martindale, M.Q., Baxevanis, A.D., and NISC Comparative Sequencing Program (2010). The homeodomain complement of the ctenophore *Mnemiopsis leidyi* suggests that Ctenophora and Porifera diverged prior to the ParaHoxozoa. *EvoDevo* 1, 9.

Ryan, J.F., Pang, K., Schnitzler, C.E., Nguyen, A.-D., Moreland, R.T., Simmons, D.K., Koch, B.J., Francis, W.R., Havlak, P., Smith, S.A., et al. (2013). The Genome of the Ctenophore *Mnemiopsis leidyi* and Its Implications for Cell Type Evolution. *Science* 342.

Samadi, L., and Steiner, G. (2010). Conservation of ParaHox genes' function in patterning of the digestive tract of the marine gastropod *Gibbula varia*. *BMC Dev. Biol.* 10, 74.

Shimizu, T., Bae, Y.-K., Muraoka, O., and Hibi, M. (2005). Interaction of *Wnt* and *caudal*-related genes in zebrafish posterior body formation. *Dev. Biol.* 279, 125–141.

Shinmyo, Y., Mito, T., Matsushita, T., Sarashina, I., Miyawaki, K., Ohuchi, H., and Noji, S. (2005). *caudal* is required for gnathal and thoracic patterning and for posterior elongation in the intermediate-germband cricket *Gryllus bimaculatus*. *Mech. Dev.* 122, 231–239.

Skromne, I., Thorsen, D., Hale, M., Prince, V.E., and Ho, R.K. (2007). Repression of the hindbrain developmental program by Cdx factors is required for the specification of the vertebrate spinal cord. *Dev. Camb. Engl.* 134, 2147–2158.

Smith, F.W., Boothby, T.C., Giovannini, I., Rebecchi, L., Jockusch, E.L., and Goldstein, B. (2016). The Compact Body Plan of Tardigrades Evolved by the Loss of a Large Body Region. *Curr. Biol.* 26, 224–229.

Tomlinson, S.G. (1987). Intermediate Stages in the Embryonic Development of the Gastropod *Ilyanassa obsoleta*: a Scanning Electron Microscope Study. *Int. J. Invertebr. Reprod. Dev.* 12, 253–280.

Vellutini, B.C., Martín-Durán, J.M., and Hejnol, A. (2017). Cleavage modification did not alter blastomere fates during bryozoan evolution. *BMC Biol.* 15, 33.

Wollesen, T., Rodríguez Monje, S.V., McDougall, C., Degnan, B.M., and Wanninger, A. (2015). The ParaHox gene *Gsx* patterns the apical organ and central nervous system but not the foregut in scaphopod and cephalopod mollusks. *EvoDevo* 6.

Wollesen Tim, Rodríguez Monje Sonia Victoria, Luiz de Oliveira André, and Wanninger Andreas (2018). Staggered Hox expression is more widespread among molluscs than previously appreciated. *Proc. R. Soc. B Biol. Sci.* 285, 20181513.

Wu, L.H., and Lengyel, J.A. (1998). Role of *caudal* in hindgut specification and gastrulation suggests homology between *Drosophila* amnioproctodeal invagination and vertebrate blastopore. *Development* 125, 2433–2442.

Wysocka-Diller, J., Aisemberg, G.O., and Macagno, E.R. (1995). A novel homeobox cluster expressed in repeated structures of the midgut. *Dev. Biol.* 171, 439–447.

Young, T., Rowland, J.E., van de Ven, C., Bialecka, M., Novoa, A., Carapuco, M., van Nes, J., de Graaff, W., Duluc, I., Freund, J.-N., et al. (2009). Cdx and Hox Genes Differentially Regulate Posterior Axial Growth in Mammalian Embryos. *Dev. Cell* 17, 516–526.